Bulletin of Engineering Geology and the Environment (2019) 78:3159–3174
https://doi.org/10.1007/s10064-018-1337-z

ORIGINAL PAPER

Integrated approach for determining spatio-temporal variations in the hydrodynamic factors as a contributing parameter in landslide susceptibility assessments

Mustafa Can Canoglu[1] · Hüsnü Aksoy[2] · Murat Ercanoglu[3]

Received: 12 February 2018 / Accepted: 26 June 2018 / Published online: 6 July 2018

Abstract
Although general approaches to the effect of water on the mechanisms causing landslides have been adopted, the work presented in this paper was carried out to quantify the landslide susceptibility variation in space and time, integrating the soil moisture distribution and routing (SMDR) model and landslide susceptibility concept. The approach proposed in the present study reflects the temporal effects of the saturation degree index (SDI) on landslide susceptibility as a new index to understand the effect of soil saturation. The topographic wetness index (TWI) is a conventional parameter that represents the relative wetness on landsliding. The new proposed landslide susceptibility approach is used in the study area to understand the effect of soil saturation and the emergence of the Derebaşı landslide in the study area. The comparative results of landslide susceptibility maps obtained from the new approach utilizing the proposed SDI and conventional TWI are remarkable. Accordingly, a new substantial method is proposed using the attainable monthly mean meteorological data to generate monthly landslide susceptibility maps. The results obtained for the Derebaşı landslide using the proposed method are validated with the other landslide that has occurred in the same watershed. The results revealed that the approach proposed in this study was compatible with the landslide mechanism in the study area and may help to express the water effect in landslide susceptibility analyses.

Keywords Landslide susceptibility · Saturation degree · Frequency ratio analysis · Soil moisture distribution and routing · Karabük-Yenice

Introduction

There is an increasing interest in landslide susceptibility assessments in many areas of the world. Landslide susceptibility mapping has become essential to manage land use and built-up areas. Many methods and techniques have been proposed to evaluate where landslides are most likely to occur using geographic information systems (GIS) and quantitative methods (Süzen and Doyuran 2004; Ercanoglu and Gokceoglu 2004; Ercanoglu 2005; Guzzetti et al. 2005; Süzen and Kaya 2012; Çölkesen et al. 2016; Ko and Lo 2016; Mead et al. 2016; Tsangaratos and Ilia 2016). Landslides are the result of interdependent spatio-temporal processes, including static and dynamic factors. Static factors (e.g., elevation, slope, aspect, topographical curvature, topographic wetness index, etc.) vary spatially and remain steady temporally. Dynamic (triggering) factors (e.g., earthquakes, precipitation, human activities, soil moisture) vary temporally and remain spatially steady at the watershed scale. The aim of this study was to evaluate the water effect in the vadose zone by considering the landslide susceptibility concept with integration of the saturation degree index (SDI).

The study area is in the western part of the Black Sea Region (Turkey), which is infamous as the most landslide-prone region in the country. Landslides in this region have been studied by many researchers (Temiz 2000; Ercanoglu and Gokceoglu 2002, 2004; Ercanoglu 2003; Ercanoglu et al. 2004; Canoglu 2015). In these studies, landslide susceptibility of this region was assessed and compared by different methodologies, such as fuzzy logic

✉ Mustafa Can Canoglu
mccanoglu@sinop.edu.tr

[1] Faculty of Engineering and Architecture, Environmental Engineering Department, Sinop University, 57000 Sinop, Turkey

[2] Faculty of Engineering, Civil Engineering Department, Atılım University, İncek, Ankara, Turkey

[3] Faculty of Engineering, Geological Engineering Department, Hacettepe University, Beytepe, Ankara, Turkey

and statistical analyses, since this region was known as one of the most landslide-prone areas of Turkey. In almost every study, it was highlighted that the main triggering factor for the landslides was rainfall, but it was not analyzed and its effect was not taken into consideration. In this region, none of the landslides was triggered by earthquakes (based on the archives and seismic records) or human activities. Many researchers have noted that, in general, landslides occur after excessive rainfall (Ayalew 1999; Calcaterra et al. 2000; Kuthari 2007; Giannecchini et al. 2012). However, the Derebaşı landslide, which occurred in the study area, was not caused by excessive rainfall. On the date on which the Derebaşı landslide occurred (5 June 2000), the amount of rainfall recorded by Yenice Meteorological Station, situated very close to the landslide location, was only 7.3 mm. In addition, no seismic activity was recorded at or just before the occurrence date and any trace of human effect (mining, road construction, etc.) was not observed. For this reason, one of the major goals of this study was to evaluate why the Derebaşı landslide occurred using spatio-temporal saturation degree variations in order to reveal the initiation mechanism of this landslide.

The topographic wetness index (TWI) is a commonly used index to reflect the effect of water in landslide susceptibility assessments. Moore et al. (1991) defined the TWI as an indicator of the spatial distribution of soil water content, as expressed in Eq. (1):

$$\mathrm{TWI} = \ln\left(A/\tan\theta\right) \tag{1}$$

where A is the specific catchment area and θ is the local slope. However, this index is valid under steady-state meteorological conditions and is not representative for rainfall-runoff processes. For example, let us consider two watersheds, namely WS1 and WS2, with the same topographical features. WS1 is located in a desert climate region and WS2 in an Amazon climate region, and, in such a case, the TWIs of WS1 and WS2 will be the same. But in reality, the wetness conditions and the effect of water on the slopes with respect to landslide mechanisms will be completely different. Under this circumstance, the TWI cannot exactly reflect the dynamic and static processes of landslide susceptibility. To reflect the spatio-temporal effect of hydrodynamic factors, a new index should be integrated into the landslide susceptibility assessments. Therefore, in this study, a model was proposed that includes the spatial and temporal variation of the soil moisture in terms of a new index reflecting the spatio-temporal effect of water.

The soil moisture and landslide relationship has been tackled by many researchers (Pelletier et al. 1997; Pack et al. 1998; Van Asch et al. 1999; Ray et al. 2010a, 2010b, 2011). However, these studies are not landslide susceptibility studies and consist of a conventional slope stability approach combining a factor of safety with a hydrologic model. Gorsevski et al. (2006) and Canoglu (2017) studied a spatio-temporal landslide susceptibility concept with the use of a hydrologic model based upon the saturation excess runoff phenomenon. However, in these studies, a factor of safety concept was considered and expressing landslide susceptibility through a factor of safety is beyond the philosophy of the landslide susceptibility concept. For this reason, in order to address the lack of consideration of an index representing the spatial and temporal effects of the water in landslide susceptibility assessments, the soil moisture distribution and routing (SMDR) model is executed (Soil and Water Laboratory 2003). The SMDR is a fully spatially distributed model, based on the saturation excess runoff phenomenon where the soil hydrodynamic processes are captured in each pixel of the selected watershed. By processing the SMDR model, a map of the degree of saturation has been obtained for the date of the landslide. With the aim of integrating the effect of water in the landslide susceptibility concept, the saturation degree map was converted to a new index, namely the SDI, by the frequency ratio analysis method proposed by Lee and Talib (2005).

For the execution of the SMDR model, digital maps such as a digital elevation model (DEM), aspect map, vegetative characteristic map (VCM), soil type map (STM), and watershed boundary map (WBM), as well as ASCII look-up tables such as the vegetative characteristics table (VCT), soil characteristics table (SCT), and meteorological data tables, are required. STM and SCT were obtained from the laboratory tests applied on ten representative soil samples collected from the watershed area.

The work presented here is aimed at determining the effect of water on landslide susceptibility considering spatio-temporal processes. The SDI is generated from monthly mean meteorological data for 12 months by combining the SMDR model and frequency ratio analysis. The SDI were produced for 12 months and used for the generation of monthly landslide susceptibility maps covering a time period of one year. In this way, landslide susceptibility was determined from the temporal perspective and it became possible to follow the variations of the landslide susceptibility during the considered period. Concisely, this study includes four stages: (a) simulating the saturation degree map of the Yenice watershed for the date of occurrence of the Derebaşı landslide by processing the SMDR model, (b) generating an SDI map using frequency analysis, (c) comparing the landslide susceptibility maps rendered by the TWI and SDI, and (d) generating landslide susceptibility maps for 12 months (considered period) using the SDI with monthly mean meteorological data.

General characteristics of the study area

The study area is located in the West Black Sea Region of Turkey and covers an area of 15.34 km^2. The climate is of oceanic type with high and evenly distributed rainfall all year round according to the Köppen (1936) climate classification. Summers are warm and humid; winters are cool and damp (Atalay 1997). The Black Sea is the region that receives the greatest amount of precipitation in Turkey. Snowfall is quite common between the months of December and March, lasting for a week or two, and can be heavy. The study area, called the Yenice watershed, is located approximately 26 km west of Karabük city (see Fig. 1). Landslides in the Yenice watershed have been frequently reported in some studies (Ercanoglu 2003; Ercanoglu and Gokceoglu 2004; Alkevli 2009). According to these studies, the Yenice watershed is covered by the Ulus Formation, which is of Upper Cretaceous age. The Ulus Formation represents a typical flysch sequence that is highly susceptible to weathering (Deveciler 1986; Demir and Ercan 1999). Although the term flysch refers to "rock material", the landslides in the study area occur within the weathering zone of flysch layers. In other words, landslides in the region occur in the zone of soil type material (Ercanoglu 2005). In order to determine the site characteristics of the watershed and soil sampling, detailed field work was performed. During the field studies carried out in the Yenice watershed, four different soil types were observed and mapped. In accordance with the sieve analysis realized on the soil samples taken from the field, clay (C), clayey loam (CL), loam (L), and sandy clay (SC) soil types were obtained. According to the VCM acquired by the Directorate of Yenice Regional Forestry for the date on which the Derebaşı landslide occurred, 20.3% of the area of the Yenice watershed was covered by forest. On the basis of field observations, the morphometric size parameters of the Derebaşı landslide are width ~ 300 m and length ~ 850 m. The approximate depth of the slip surface is around 30 m, as determined from the field observations. Elevations in the area range between 165 and 837 m and the highest point in the study area is Sepetçi Ridge. There is also an important topographic feature in the form of Tepetarla Ridge (see Fig. 2). In the Yenice watershed, the slope angles range between 0° and 41°, with an average of 19°. The slope at the Derebaşı landslide location ranges between 19° and 31°. Farmlands exist on gentle slopes, while extensive and thick forests cover the highest and steepest elevations. Çobanköy, Derebaşı, Mısıroglu, and Beşevliler are the main districts of the study area.

Based on the information gathered from the Republic of Turkey Prime Ministry Disaster and Emergency Management Presidency, the exact date of the Derebaşı landslide was 5 June 2000. Although the exact date of the Cebeciler landslide was not recorded, the year was reported as 1998. The Yenice watershed embodies many landslides besides the Derebaşı and Cebeciler landslides, but the proposed methodology focuses on the Derebaşı landslide and validation of the proposed methodology is conducted using the Cebeciler landslide (Fig. 1). This study was focused on the Derebaşı and Cebeciler landslides because the only known dates of landslides in this region were the Derebaşı (daily scale) and Cebeciler (semi-monthly scale) landslides.

Input data and data production

Within the context of the study, field work and sampling, laboratory tests, execution of the SMDR model, and implementation of frequency ratio analysis were realized in order to identify the weight of the saturation degree on the landslide susceptibility. For the execution of the SMDR model, five raster maps (the DEM, STM, VCM, WBM, and aspect map) and four ASCII look-up tables (VCT, SCT, PDF, and daily meteorological table) are required. Frequency ratio analysis was carried out with six variables (topographic elevation, slope, aspect, SDI or TWI, permeability, and soil type).

The DEM of the study area is generated by digitizing the 1:25000 scaled topographical map of the General Command of Mapping (National Mapping Agency of Turkey 1999). The resolution of the DEM was 10 m × 10 m. The aspect map, slope map, and WBM were generated by the Spatial Analyst Tool of the ArcGIS 10.1 software. The VCM (for the year 2000), VCT, and plant development factor (PDF) were obtained from the Directorate of Yenice Regional Forestry. The STM was drawn based on the field observations and laboratory tests (grain size distribution). The first step in determining the STM borderlines is mapping the soil type variations based on the field observations and collection of ten representative soil samples from the watershed (Fig. 2).

Subsequently, laboratory tests were performed on the soil samples, the grain size distribution was determined for each sample, and the inverse distance weighting (IDW) algorithm was utilized to obtain the percentage map for clay, silt, and sand, respectively. Finally, the borderline of the STM was drawn by observations and interpolation. Then, the STM was re-drawn based on the field observations and verified by the IDW. The required soil properties for the SCT were compiled from the laboratory tests and were estimated from the soil texture through statistical relationships proposed by Rawls and Brakensiek (1983, 1985). The daily meteorological table was obtained from the General Directorate of Meteorological Service of Turkey for Yenice Station for the years 1989–2009. The monthly mean precipitation, daily temperature, and monthly potential evapotranspiration (PET) are tabulated in Table 1 for each month.

The permeability map was obtained by interpolating the results of the permeability test (ASTM standard D5084 2010) carried out on the soil samples. Then, the permeability map was determined by the IDW method. Furthermore, due to the anomaly of saturation degree around the crown of the Derebaşı landslide, the landslide area was divided into three zones to observe the initiation location (see Fig. 2).

Methodology

In fact, the past and present are key to the future, a very well known uniformitarianism principle, based on the idea that events

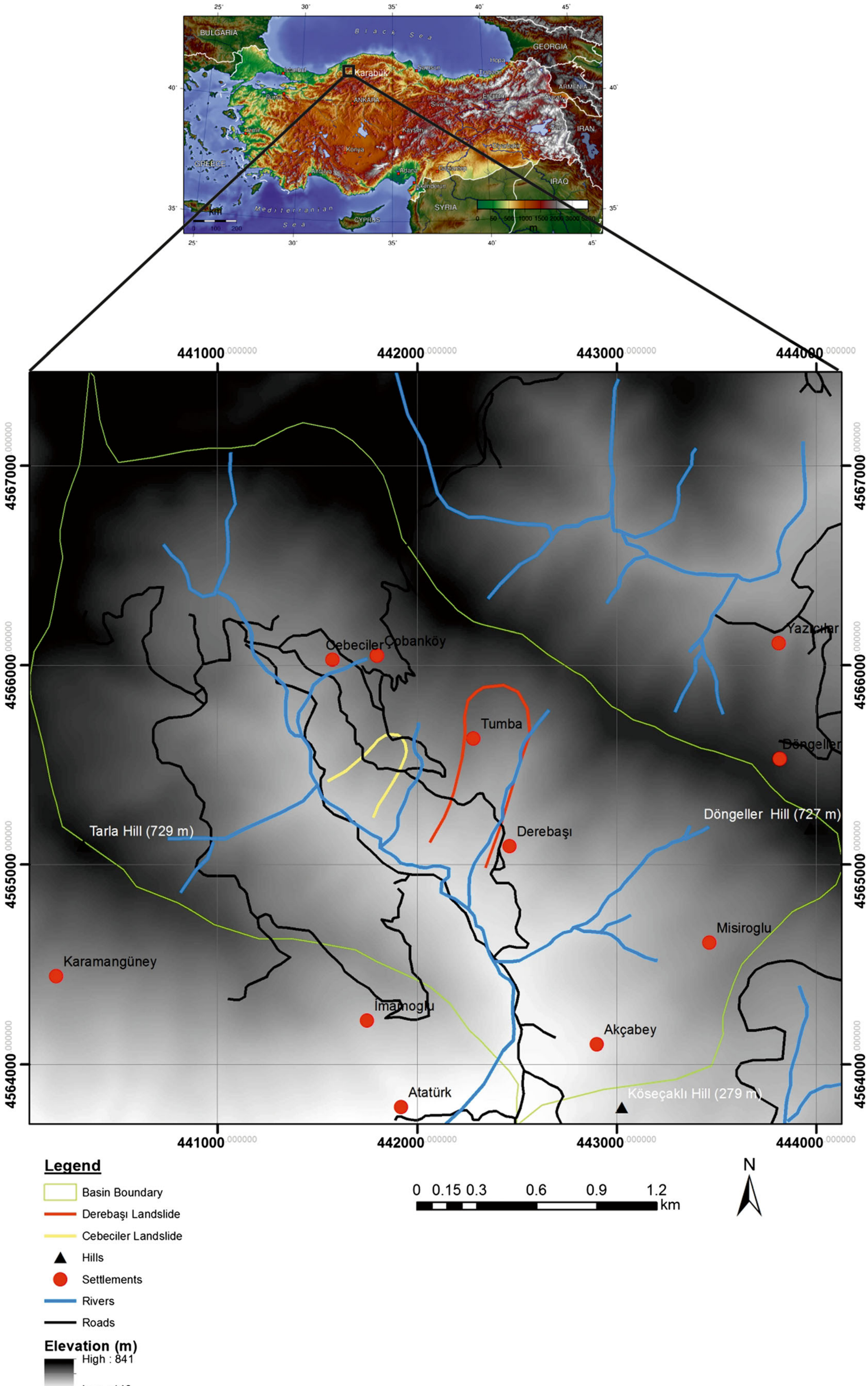

Fig. 1 Location map of the study area

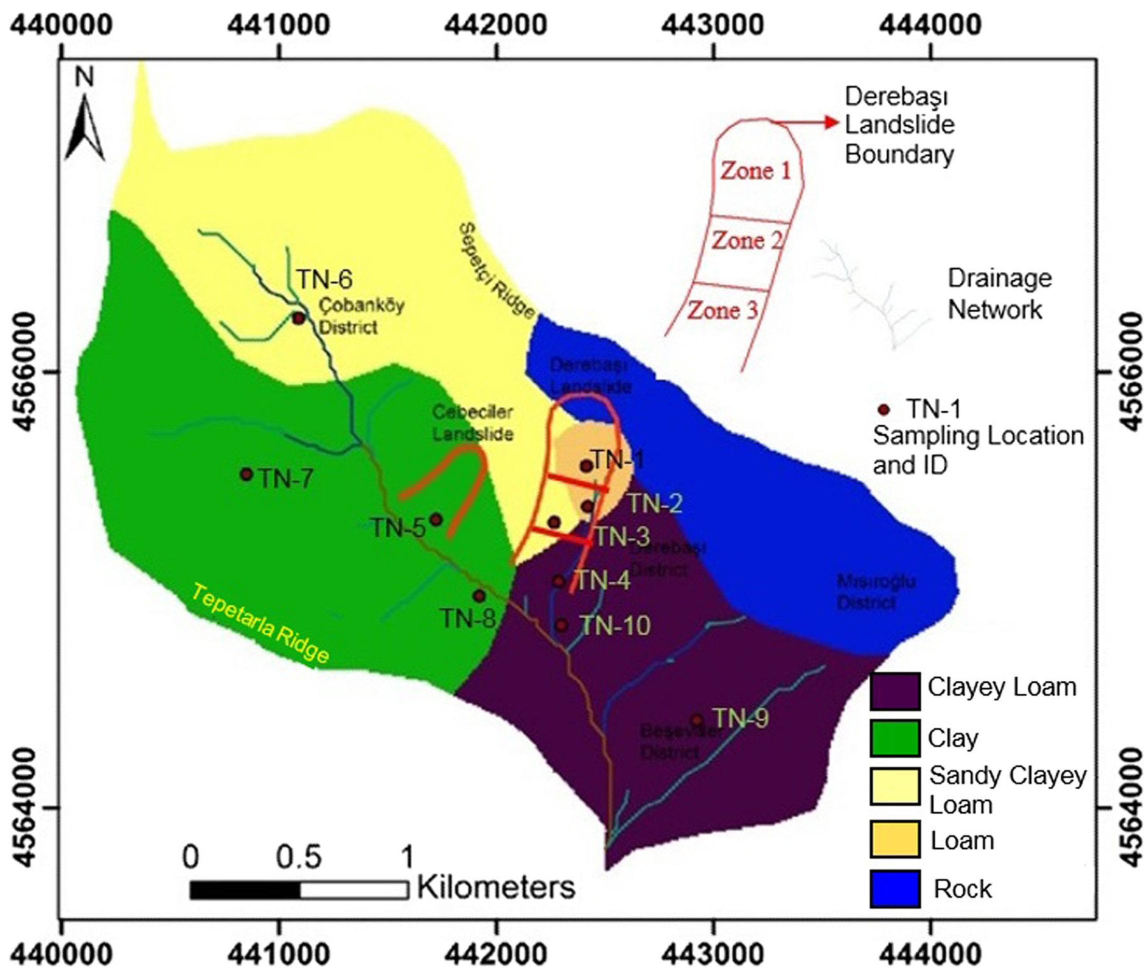

Fig. 2 Soil type map of the Yenice watershed

in the future will be more likely to occur under the similar conditions that led to the past and present (Van Westen et al. 2008). In harmony with the purpose of the study, the SMDR model and frequency ratio analysis approaches were utilized. The SMDR model was employed to generate the saturation degree map for the date on which the Derebaşı landslide occurred. On the SDI map of the Yenice watershed, frequency ratio analysis was carried out to assess landslide susceptibility. Saturation degree maps were obtained by the SMDR model. These maps were analyzed and categorized by the frequency ratio method in order to obtain the SDI. The final stage of the methodology consists of the generalization of the suggested model for the landslides of unknown date by taking into consideration the available monthly mean meteorological data.

Table 1 Mean meteorological data (1989–2009)

	Monthly precipitation (mm)	Daily temperature (°C)	Monthly PET (mm)
January	44.2	4.8	0
February	41.8	5.6	0
March	40.4	8.7	0
April	49.2	12.7	96
May	42.9	16.6	144
June	56.9	20.6	144
July	27.6	23.5	207
August	37.2	23.5	135
September	35.0	19.1	84
October	49.5	14.9	42
November	57.8	8.8	0
December	50.8	5.4	0

PET, potential evapotranspiration

SMDR model

The general purpose of the SMDR model is to identify the location and evolution of variable source areas for runoff generation and to estimate the saturation degree from the water fluxes. Therefore, it does not require extensive calibration and is designed to use data that are readily available in electronic form (Gérard-Marchant et al. 2006).

In this study, the SMDR model divides the watershed into a square grid of cells with cell dimensions of 10 m ×

10 m. Larger cell dimensions tend to misrepresent the landscape curvatures and lead to unreasonably high estimates of soil water content (Kuo et al. 1999). Within each cell, soil properties are assumed to be homogeneous. A soil water mass balance is computed for the surface soil of each cell at each time step. A daily time step is chosen, considering the computational speed, accuracy of results, and data availability. The water mass balance calculation is realized by the SMDR model within a defined watershed boundary. The daily water inputs considered by the SMDR model for each cell are the daily precipitation and lateral flow from the surrounding upslope cells. The outputs are lateral flow to the surrounding downslope cells, percolation, and evapotranspiration. The water mass balance equations for each cell are expressed in the SMDR model as follows:

$$W^2\ |\Theta(t)-\Theta\ (t-\Delta t)| = |RF(t)+SM(t)| + Qi\ (t)-Qo(t)-ET\ (t)-P(t)-SE(t) \qquad (2)$$

where W is the grid size (m), is the cell average water content (cm^3.cm^{-3}), Δt is the time step (days), RF and SM are the rainfall and snowmelt volumes, respectively, Q_i is the volume of water received through lateral flow from the surrounding upslope cells, Q_o is the volume of water lost through lateral flow to the surrounding downslope cells, ET is the volume of water lost by evapotranspiration, P is the volume of water lost by percolation, and SE is the saturation excess runoff. For this equation, the thickness of the soil is taken as 1 m. Volumes are expressed in cubic meters.

The daily mean air temperature is corrected by the adiabatic lapse rate of 6.5×10^{-3} for changes in local elevation (Boll et al. 1998). Precipitation occurring when the mean daily temperature is below 0 °C is assumed to be snow. Snow is assumed to remain melted until the mean daily temperature is above 0 °C. The SM is computed by a simple land-cover-dependent temperature index method. Meteorological data defined for the SMDR model are assumed to be the same for each pixel in the watershed.

Subsurface lateral flow is calculated for each cell using Darcy's law by approximating the hydraulic gradient by the local slope (β). Lateral outflow (Q_o) can be expressed as follows:

$$Q_o = -\kappa\, K(\Theta)\ \ W\, \beta\, \Delta t \qquad (3)$$

where K is the average hydraulic conductivity of the layer (m.day^{-1}) and κ is a depth-dependent multiplier (typical range of 2–10) introduced to correct transmissivities for preferential flows in macropores (Boll et al. 1998). In the SMDR model, the average hydraulic conductivity K is defined as:

$$\begin{aligned} &K(\Theta) = 0 && for\ \Theta < \Theta_f \\ &K(\theta) = \mathrm{K_{sat}}.\exp\left(\alpha\frac{(\theta-\theta s)}{(\theta s-\theta_f)}\right) && for\ \Theta_f \le \Theta < \Theta_m \\ &K(\Theta) = K_m + K_s\frac{(\theta-\theta m)}{(\theta s-\theta_m)} && for\ \Theta_m \le \Theta \end{aligned} \qquad (4)$$

where Θ_f, Θ_m, and Θ_s correspond to the field capacity, macroporous drainage limit, and saturation, respectively. On the other hand, $K_s = K(\ _s)$ and $K_m = K(\ m)$ are the hydraulic conductivities at saturation and at the macroporous drainage limit, respectively, and α is a universal constant equal to 13 for a large range of soils (Bresler et al. 1978; Steenhuis and van der Molen 1986). The D∞ algorithm was employed to find the distribution of the lateral outflows from each cell according to the local aspect between one cardinal and one diagonal downslope neighboring cell (Tarboton 1997). The sum of the contributions received from the upslope surrounding cells is considered as lateral inflow. Additionally, in the SMDR model, the soil type variation within the watershed affects only hydraulic conductivity, which is one of the parameters controlling the lateral flow rate (Eq. 3). The lateral flow rate is a component of water mass balance calculation of each cell for a defined time step (Eq. 2). For this reason, the accuracy of the saturation degree maps obtained from the SMDR model cannot be affected by the soil type distribution within the watershed.

In the SMDR model, evapotranspiration is calculated as a function of the daily PET, vegetation condition, and soil moisture according to Thornthwaite and Mather (1955). Basically, the ratio between the actual and PET increases linearly with water content from zero at or below the permanent wilting point, Θ_{pwp}, to a value of one at or above the ET limit, Θ_{etl}.

Determining the percolation amount requires some knowledge of the fracture properties of rock material. Therefore, the soil below the bounding layer is modeled as a lumped subsurface reservoir and the total percolating volume is added to the reservoir storage at each time step. In the SMDR model, percolation is calculated for each cell as follows:

$$P = min[K(\Theta); K_{sub}]W^2\ \Delta t \qquad (5)$$

where K_{sub} is the conductivity at saturation of the cell substratum (m.day^{-1}) and the hydraulic conductivity K is given by Eq. (4). Percolation stops when the average water content of the bottom structural layer is less than the field capacity. The saturation excess overland flow SE (m^{-3}) is constituted by the water in excess of saturation for the end of each time step.

The SMDR model results for the date of occurrence shows an anomaly of saturation degree around the crown

Table 2 Number of pixels (frequency) for each saturation degree class of three different zones between the dates 25 May 2000 and 5 June 2000 obtained from the soil moisture distribution and routing (SMDR) model

Date	Rainfall (mm)	Temperature (°C)	ET (mm)	Saturation degree			
				Class	Frequency zone 1	Frequency zone 2	Frequency zone 3
25.05.2000	23.1	15.2	1	0.70–0.75	1	0	0
				0.75–0.80	2	0	0
				0.80–0.85	322	322	393
				0.85–0.90	721	379	446
				0.90–0.95	1	0	0
				0.95–1.00	0	0	0
26.05.2000	2.9	17.1	1	0.70–0.75	0	0	0
				0.75–0.80	4	0	0
				0.80–0.85	374	385	430
				0.85–0.90	668	316	409
				0.90–0.95	1	0	0
				0.95–1.00	0	0	0
27.05.2000	3.3	20.3	4.3	0.70–0.75	0	0	0
				0.75–0.80	4	0	0
				0.80–0.85	439	433	472
				0.85–0.90	600	268	367
				0.90–0.95	3	0	0
				0.95–1.00	1	0	0
28.05.2000	0.5	20	5.5	0.70–0.75	2	0	0
				0.75–0.80	5	0	0
				0.80–0.85	464	453	496
				0.85–0.90	567	248	343
				0.90–0.95	8	0	0
				0.95–1.00	1	0	0
29.05.2000	1.4	22.7	6.4	0.70–0.75	2	0	1
				0.75–0.80	11	0	6
				0.80–0.85	482	471	520
				0.85–0.90	540	230	312
				0.90–0.95	12	0	0
				0.95–1.00	0	0	0
30.05.2000	1.6	18.2	4.4	0.70–0.75	1	1	1
				0.75–0.80	12	4	8
				0.80–0.85	508	484	544
				0.85–0.90	512	212	286
				0.90–0.95	13	0	0
				0.95–1.00	1	0	0
31.05.2000	0.9	18.7	3.4	0.70–0.75	2	1	1
				0.75–0.80	13	8	13
				0.80–0.85	512	490	547
				0.85–0.90	501	200	278
				0.90–0.95	17	2	0
				0.95–1.00	2	0	0
01.06.2000	0	20.8	3.4	0.70–0.75	2	1	1
				0.75–0.80	24	16	22
				0.80–0.85	520	488	550

Table 2 (continued)

Date	Rainfall (mm)	Temperature (°C)	ET (mm)	Saturation degree			
				Class	Frequency zone 1	Frequency zone 2	Frequency zone 3
				0.85–0.90	478	192	265
				0.90–0.95	21	4	1
				0.95–1.00	2	0	0
02.06.2000	2.5	16.2	5.4	0.70–0.75	4	1	1
				0.75–0.80	33	28	40
				0.80–0.85	536	480	539
				0.85–0.90	447	184	257
				0.90–0.95	22	8	2
				0.95–1.00	5	0	0
03.06.2000	11.2	15.1	1.5	0.70–0.75	6	1	1
				0.75–0.80	43	38	64
				0.80–0.85	538	478	518
				0.85–0.90	429	172	251
				0.90–0.95	25	12	5
				0.95–1.00	6	0	0
04.06.2000	10.7	17.3	1.8	0.70–0.75	9	2	3
				0.75–0.80	52	57	90
				0.80–0.85	532	457	493
				0.85–0.90	415	172	247
				0.90–0.95	31	13	6
				0.95–1.00	8	0	0
05.06.2000	7.3	19.6	2.1	0.70–0.75	10	1	6
				0.75–0.80	68	79	119
				0.80–0.85	523	436	468
				0.85–0.90	399	164	237
				0.90–0.95	37	21	9
				0.95–1.00	10	0	0

ET, evapotranspiration

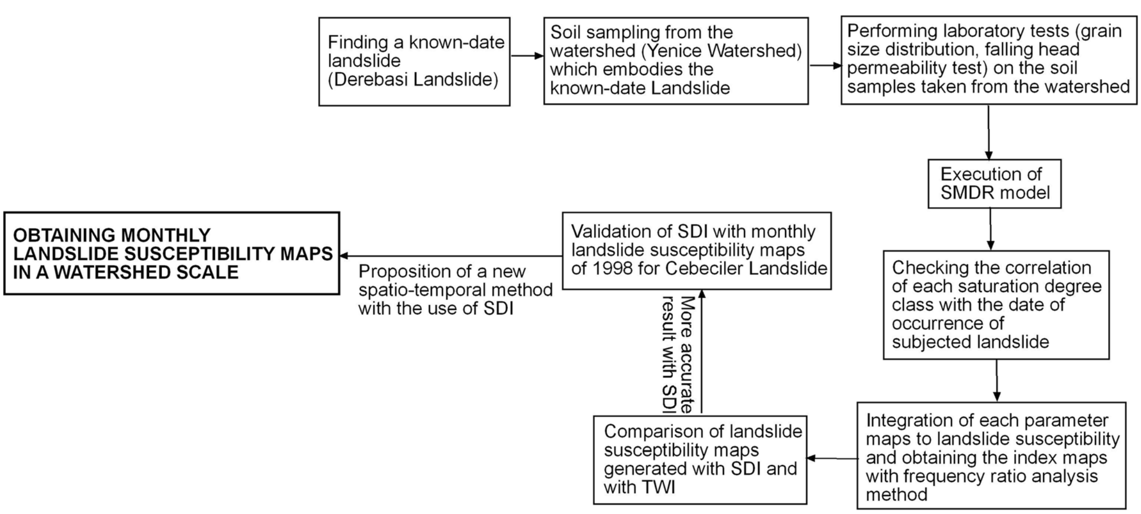

Fig. 3 Workflow diagram summarizing the followed methodology

of the Derebaşı landslide. For this reason, the Derebaşı landslide area is divided into three zones in order to observe the initiation location (see Fig. 2). Saturation degree maps between the dates of 25 May and 5 June 2000 obtained from the SMDR model are analyzed for three different zones of the Derebaşı landslide to follow up the landslide evolution in space and time (Table 2).

The number of pixels (frequency) of each saturation degree class is analyzed from 10 days before the date of occurrence of the Derebaşı landslide. The increase in the number of pixels in zone 1 for the saturation degree classes 0.90–0.95 and 0.95–1.00 were more remarkable (see Table 2). This prominent increase indicates that the Derebaşı landslide was initiated from zone 1, as reported by the Disaster and Emergency

Table 3 Spatial relationships between each parameter and landslide and frequency ratio values

Parameters	Class	Number of pixels without landslide	Ratio a (%)	Number of pixels with landslide	Ratio b (%)	Frequency ratio (b/a)
Slope (°)	0–10	7374	9.74	0	0.00	0.00
	10–20	32,825	43.36	151	14.39	0.33
	20–30	31,744	41.93	896	85.41	2.04
	> 30	3756	4.96	2	0.19	0.04
Aspect (°)	0–45	5360	7.08	0	0.00	0.00
	45–90	12,912	17.06	0	0.00	0.00
	90–135	8081	10.68	11	1.05	0.10
	135–180	10,642	14.06	696	66.35	4.72
	180–225	21,820	28.82	334	31.84	1.10
	225–270	14,696	19.41	8	0.76	0.04
	270–315	1904	2.52	0	0.00	0.00
	315–360	284	0.38	0	0.00	0.00
Elevation (m)	150–300	9101	12.02	0	0.00	0.00
	300–450	19,367	25.58	86	8.20	0.32
	450–600	22,533	29.77	963	91.80	3.08
	600–750	22,334	29.50	0	0.00	0.00
	750–900	2364	3.12	0	0.00	0.00
TWI	< 16	7	0.01	0	0.00	0.00
	16–17	48,204	63.68	1	0.10	0.00
	17–18	23,745	31.37	985	93.90	2.99
	18–19	2765	3.65	63	6.01	1.64
	19–20	978	1.29	0	0.00	0.00
Soil type	Clayey loam	18,130	23.95	0	0.00	0.00
	Clay	25,342	33.48	0	0.00	0.00
	Sandy clayey loam	19,944	26.35	169	16.11	0.61
	Loam	618	0.82	615	58.63	71.81
	Rock	11,665	15.41	265	25.26	1.64
Saturation degree (for 05.06.2000)	0.70–0.75	1281	1.69	12	1.14	0.68
	0.75–0.80	10,014	13.23	68	6.48	0.49
	0.80–0.85	36,291	47.94	523	49.86	1.04
	0.85–0.90	24,575	32.46	399	38.04	1.17
	0.90–0.95	3168	4.18	37	3.53	0.84
	0.95–1.00	370	0.49	10	0.95	1.95
Permeability ($\times 10^{-5}$ m/s)	1.64–3.40	13,954	18.43	0	0.00	0.00
	3.40–5.16	16,628	21.97	0	0.00	0.00
	5.16–6.93	38,724	51.16	0	0.00	0.00
	6.93–8.69	6300	8.32	633	60.34	7.25
	8.69–10.50	93	0.12	416	39.66	322.79

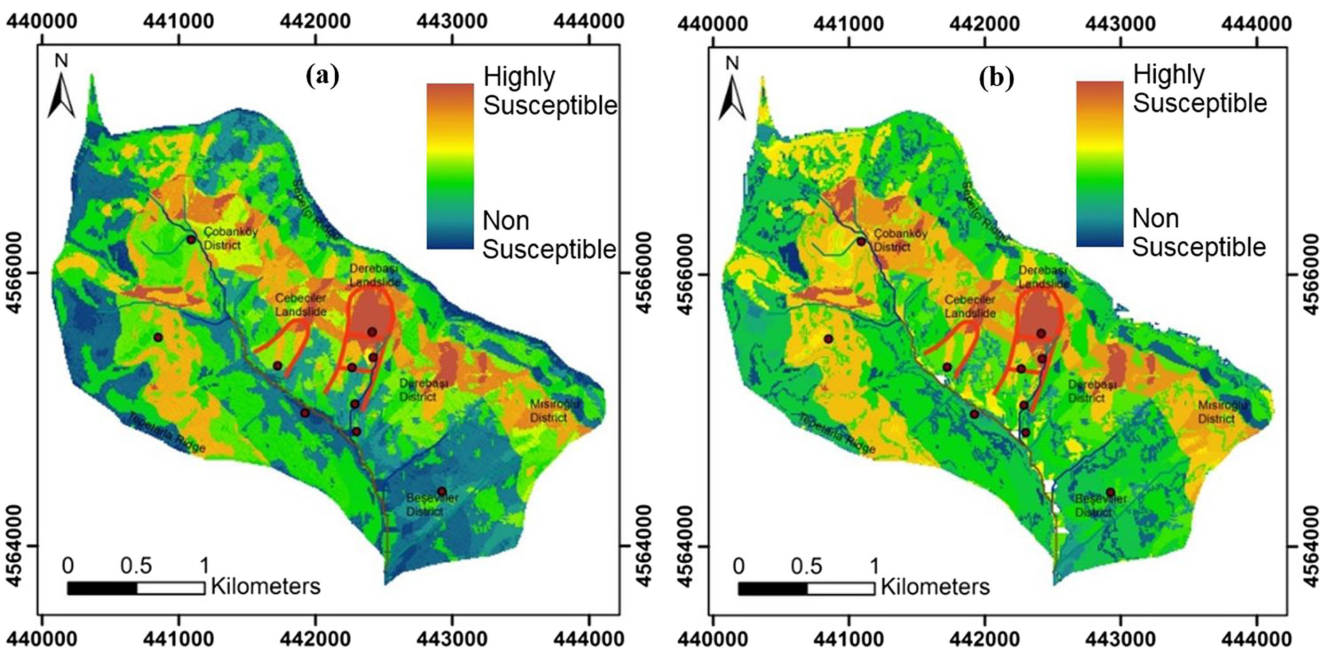

Fig. 4 Comparison of the landslide susceptibility maps of the Yenice watershed: **a** computed by Eq. 6 with the use of the saturation degree index (SDI); **b** computed by Eq. 7 with the use of the topographic wetness index (TWI)

Management Presidency archives and interviews of local people (General Directorate of Natural Disaster 2000). Additionally, it can be observed from Table 2 that the rainfall during the analyzed period (25 May to 5 June) is not in accordance with the increase in saturation degree. The reason for the increase of saturation degree in zone 1 can be explained by the water fluxes coming from upslope cells.

Frequency ratio analysis in terms of landslide susceptibility

In general, to determine the landslide susceptibility, the causal factors of past landslide occurrences are considered to assess the initiation of landslides in the future for the same region (Chung and Fabbri 1999). To reflect statistically the conceptual relation between landslides that occurred in the past and their causal factors, frequency ratio analysis was used. The frequency ratio is the ratio of the probability of occurrence to the probability of non-occurrence of specific attributes (Lee and Talib 2005). The method followed in this study can be expressed by the workflow diagram shown in Fig. 3.

If the frequency ratio is greater than 1, the relationship between a landslide and the causal parameter's attribute will be stronger; conversely, if the ratio is less than 1, the relationship between a landslide and the causal parameter's attribute will be weaker (Lee and Talib 2005). The frequency ratio is shown in Table 2 for all parameters for each parameter class. It is known from the reports of the Disaster and Emergency Management Presidency that the Derebaşı landslide was initiated from zone 1, while zones 2 and 3 were considered to be out of the landslide area in Table 3.

The ultimate landslide susceptibility is computed from the summation of each parameter's frequency ratio values using Eqs. (6) and (7). In Eq. (6), the SDI is obtained by the integration of the saturation degree map (of 5 June 2000) handled from the SMDR model and frequency ratio analysis. To emphasize the effect of the new proposed index (SDI), only basic topographic parameters are utilized in Eqs. (6) and (7) together with the SDI and TWI, respectively. The landslide susceptibility value represents the relative susceptibility to landslide occurrence, as higher values are associated with higher landslide susceptibility.

$$\begin{aligned}\text{Landslide Susceptibility (1)} = {} & \text{Fr (slope index)} + \text{Fr (aspect index)} \\ & + \text{Fr (elevation index)} \\ & + \text{Fr (saturation degree index)} \\ & + \text{Fr (soil type index)} \\ & + \text{Fr (permeability index)}\end{aligned} \tag{6}$$

$$\begin{aligned}\text{Landslide Susceptibility (2)} = {} & \text{Fr (slope index)} \\ & + \text{Fr (aspect index)} \\ & + \text{Fr (elevation index)} \\ & + \text{Fr (TWI)} \\ & + \text{Fr (soil type index)} \\ & + \text{Fr (permeability index)}\end{aligned} \tag{7}$$

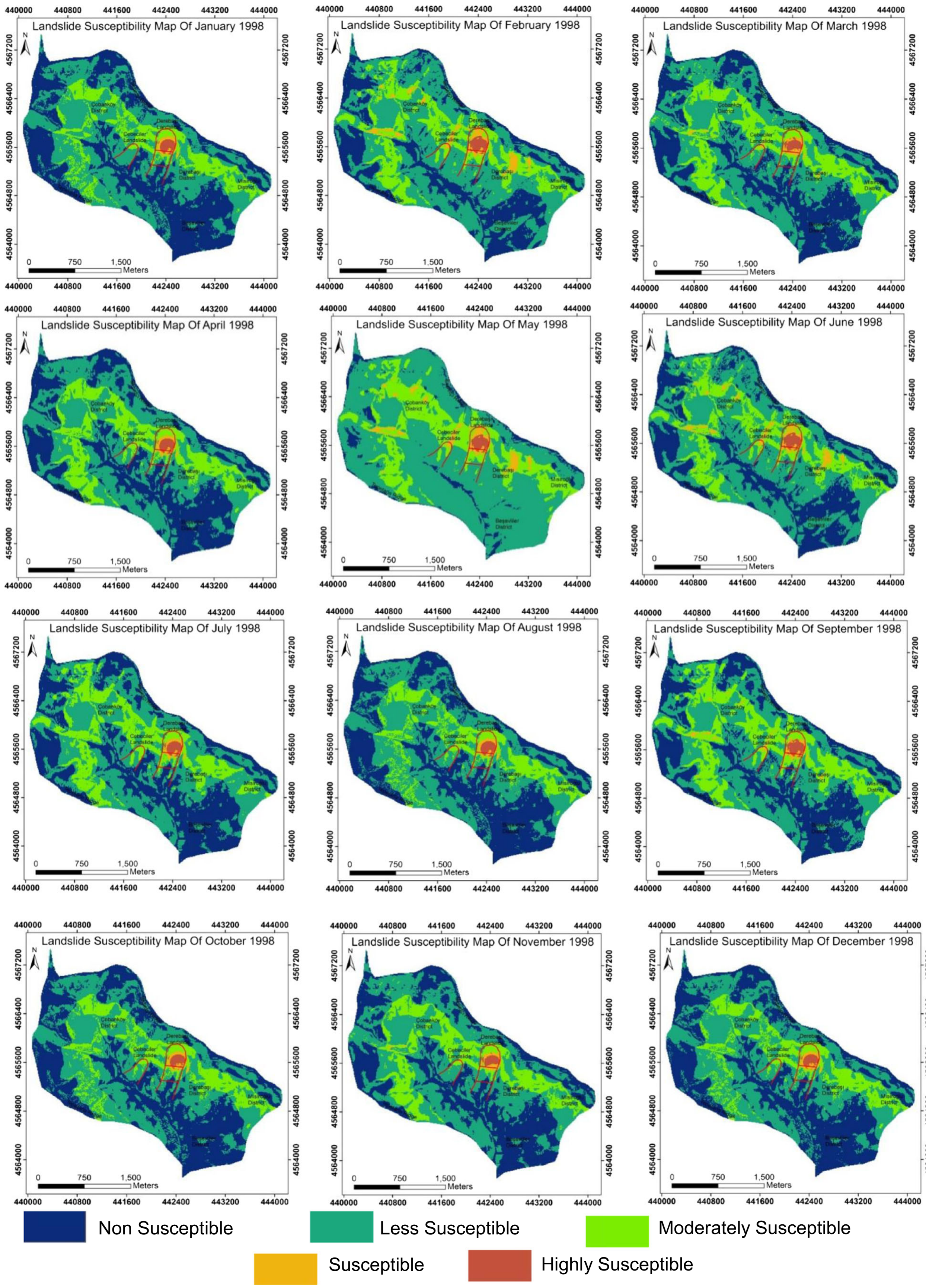

Fig. 5 Spatial patterns of monthly landslide susceptibility in the Yenice watershed for the year 1998

where Landslide Susceptibility (1) is the landslide susceptibility computed by considering the SDI, Landslide Susceptibility (2) is the landslide susceptibility computed by considering the TWI, and Fr is the frequency of each parameter for each class.

Results and discussions

To assess the results of the so-produced maps, a comparison of the landslide susceptibility maps computed by Eqs. (6) and (7) was performed. The results revealed that the effect of the SDI is more accurate for the Derebaşı landslide (Fig. 4). Furthermore, Fig. 4 shows that the Derebaşı Landslide initiated from zone 1.

Throughout this study, a new perspective on the existing landslide susceptibility concept is proposed in order to show the effect of water in terms of a new index (SDI). In other words, a new index called the SDI is considered to integrate the effect of water with the ordinary landslide susceptibility phenomenon. To validate the new proposed SDI, the same methodology is followed for the Cebeciler landslide, whose exact date of occurrence is unknown but whose year of occurrence was recorded as 1998 by the General Directorate of Natural Disaster (1998) in the geological investigation report. Therefore, monthly mean meteorological data were handled to identify landslide susceptibility maps for 12 months for the year 1998 to estimate the month in which the Cebeciler landslide occurred (Fig. 5).

In Fig. 5, landslide susceptibility classes were specified based on the natural break concept considering five different landslide susceptibility classes. It can be deduced from Fig. 5 that May was the most susceptible month in the year 1998 in the Yenice watershed for the Cebeciler landslide, as reported by the General Directorate of Natural Disaster (1998). This result illustrates that the frequency ratio analysis approach using the SDI for 12 months is also valid for the Cebeciler landslide. In addition, the percentage areas of highly susceptible and susceptible classes of February and June were greater than in the other months (Table 4).

In addition, a new procedure is considered to produce a landslide susceptibility map. This procedure utilizes the SMDR model and frequency ratio analysis in order to take into account the effect of water more determinately. Consequently, it is believed that the only initiation factor for the Derebaşı landslide is the variance of the water flux in terms of saturation degree considering the rainfall (only 7.3 mm); there was no seismic record or evidence of human activity. To create the saturation degree map of the Yenice watershed, the SMDR model based on the saturation excess runoff phenomenon was run. This study is expected to address the lack of consideration of the spatial and temporal effects of water in landslide susceptibility mapping.

The TWI is a conventional topography-based index parameter that represents the spatial variations of the effect of water in a watershed. However, it is deduced that the TWI cannot reflect hydrodynamic processes due to its representation of unclear temporal processes. Additionally, this index is proposed for determining the wetness variations of large-scale watersheds under *steady state rainfall conditions* (Moore et al. 1991). Comparison of the TWI and SDI (which is derived from the saturation degree map produced by the SMDR model for the date of occurrence of the Derebaşı landslide) indicates that the TWI map is not totally meaningful in terms of the initiation mechanism of the Derebaşı and Cebeciler landslides due to its consideration of static parameters (Fig. 6a, b).

It is seen from Fig. 6a that the TWI is in the range of 16–17 for most of the area in the Yenice watershed, and an increase of the TWI around the toe of the Derebaşı landslide can be observed, which is contrary to the initiation mechanism of the Derebaşı landslide indicated in Table 2. However, in Fig. 6b, higher values of the SDI can be observed in zone 1 of the Derebaşı landslide, in harmony with the initiation mechanism. Additionally, it

Table 4 Percentage area of each susceptibility class for each month of the year 1998

	Non-susceptible (%)	Less susceptible (%)	Moderately-susceptible (%)	Susceptible (%)	Highly susceptible (%)
January	39.53	45.33	14.04	0.56	0.54
February	27.21	50.90	18.64	2.51	0.74
March	34.34	46.85	17.48	0.79	0.54
April	35.55	46.25	17.06	0.56	0.58
May	6.49	67.72	22.38	2.67	0.74
June	28.40	51.05	17.67	2.16	0.72
July	36.13	44.44	18.34	0.52	0.57
August	40.31	45.20	13.43	0.57	0.49
September	33.24	44.46	20.75	1.04	0.51
October	39.59	45.11	14.25	0.53	0.52
November	36.04	49.77	13.03	0.68	0.48
December	38.90	45.81	14.20	0.57	0.52

can be deduced that the hydrological models based on the variable source area concept clarify the processes of the initiation of landslides in the context of landslide susceptibility phenomena more accurately.

Slope angle, slope aspect, topographical elevation, soil type, permeability, and saturation degree were used as basic topographical input parameters for the frequency ratio analysis of landslide susceptibility mapping. The SDI and the widely used TWI were employed as input maps of frequency ratio analysis and the landslide susceptibility maps were compared (see Fig. 4). Thus, it is proved that using the SDI for landslide susceptibility is more effective, deterministic, and accurate in terms of reflecting the temporal effect of water. In this way, the landslide susceptibility concept gains a temporal dimension. In other words, up until now, landslide susceptibility phenomena have answered the question of "where", while this study allows landslide susceptibility phenomenon to also approach the question of "when", similarly to the hazard concept, without executing detailed analyses.

A methodology combining the SMDR model with the frequency ratio is used to handle the landslide susceptibility maps for each month of the year 1998. The obtained landslide susceptibility maps show an anomaly in the Cebeciler landslide area, and the most susceptible month in this area is May 1998. The geological investigation report of the Cebeciler Landslide was written in May 1998. This can be evaluated as an evidence of temporal verification. Additionally, a susceptibility anomaly in the crown of the Cebeciler landslide can be evaluated as the evidence of spatial verification. Thereby, the methodology was verified spatially and temporally for a different landslide area.

The work aimed to express the SDI obtained from the methodology by combining the SMDR model with the frequency ratio mathematically. However, the static factors (e.g., elevation, slope, aspect, topographic wetness index, etc.) used for landslide susceptibility vary spatially and remain steady temporally. Dynamic (triggering) factors (e.g., earthquakes, effect of water, human activities) vary temporally and remain steady spatially at the watershed scale. It can be concluded that ignoring the static factors for a mathematical expression is inconceivable for an index that varies spatially and temporally. such as the SDI. For this reason, in order to generalize the approach shown in Fig. 5, the SMDR model executed with all the available monthly average meteorological data (1989–2009 for the Yenice watershed) and the monthly mean saturation degree maps were converted to SDI for utilization in the new generalized landslide susceptibility approach (Fig. 7).

According to the maps shown in Fig. 7, the most susceptible months were June and May, while September and November could also be considered as susceptible (Table 5). This integrated approach is promising, as it incorporates a methodology for better quantification of parameters and accurate representation of spatial and temporal landslide susceptibility. The intention of the study was to show a quantitative unbiased approach in the context of uncertainties in the effect of water as an initiation factor for landslide susceptibility. Figure 5 validates the applicability of the proposed methods, approaches, and landslide susceptibility classification index.

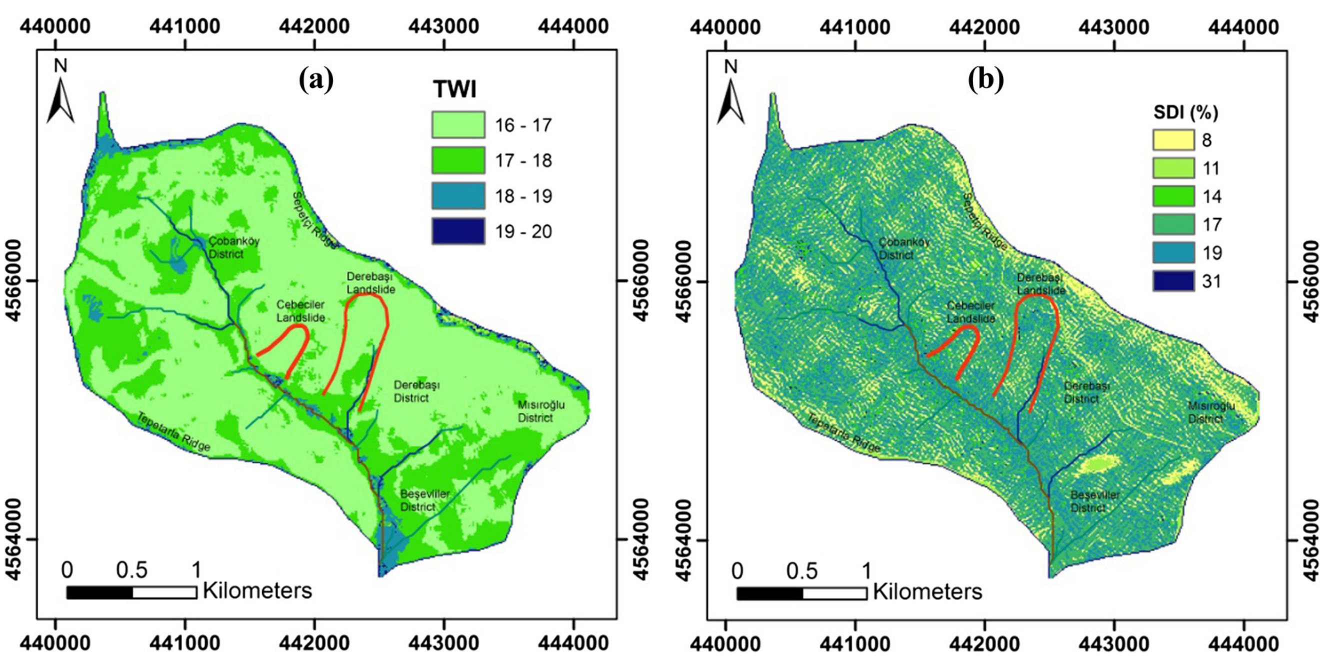

Fig. 6 Comparison of **a** the TWI and **b** the SDI for the Yenice watershed

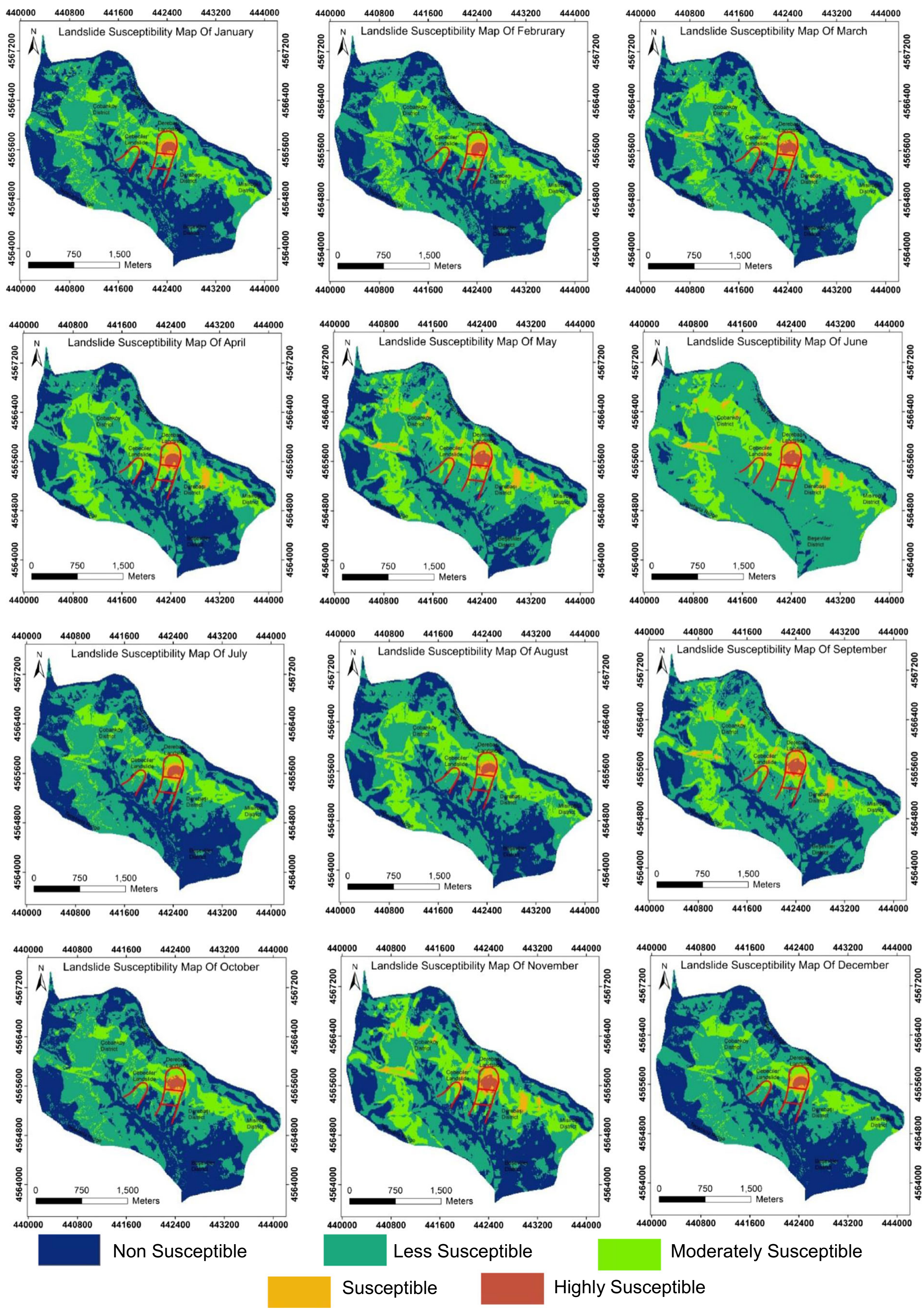

Fig. 7 Spatial patterns of monthly landslide susceptibility in the Yenice watershed

Table 5 Percentage area of each susceptibility class for each month shown in Fig. 7

	Non-susceptible (%)	Less susceptible (%)	Moderately susceptible (%)	Susceptible (%)	Highly susceptible (%)
January	41.76	45.18	12.03	0.53	0.50
February	38.94	44.98	14.98	0.54	0.56
March	33.86	50.97	13.89	0.87	0.41
April	35.35	44.21	18.30	1.55	0.59
May	27.21	50.91	18.64	2.51	0.73
June	6.49	67.72	22.38	2.67	0.74
July	40.76	47.91	10.31	0.55	0.47
August	35.25	50.54	13.15	0.61	0.45
September	28.41	51.04	17.67	2.16	0.72
October	42.51	46.25	10.24	0.53	0.47
November	34.96	42.57	19.35	2.66	0.46
December	42.34	46.31	10.35	0.53	0.47

Conclusions

Landslides are very sensitive to their triggering factor or initiation parameter. For this reason, the use of a daily scale for the proposed method could reflect the initiation mechanism of landslides more accurately, as done in the analysis of a known date landslide (Derebaşı) shown in Table 2. However, monthly mean meteorological data have been utilized to reflect the landslides which have not yet occurred for a generalized spatio-temporal landslide susceptibility method.

In this study, soil thickness in the soil moisture distribution and routing (SMDR) model is conceived as 1 m depth, and it is considered that, under this depth, the only water movement is percolation. In addition, the groundwater level is much deeper than the slip surface of the Derebaşı landslide. Therefore, groundwater fluctuations have no effect on landsliding and the vertical saturation degree variations are ineffectual for the initiation mechanism of the Derebaşı landslide. For this reason, assuming a soil thickness of 1 m for the simulation of saturation degree variations can be accepted for a landslide which has a 30-m-deep slip surface.

This method was developed to reflect the spatio-temporal effect of water on landslide susceptibility as a landslide initiation factor for a watershed that embodies a landslide. For watersheds that have no landslide generation, or in the case of the existence of significant seismic records, improvement of the stages of this method should be treated as the subject of future research studies.

Within the context of data accessibility, in countries that have soil characteristics databases, such as the SSURGO database in the United States, this method is simple and expeditious. However, in countries that do not have soil databases, the execution of this method requires site works including soil mapping and sampling and laboratory works.

References

Alkevli T (2009) Investigation of the usage of Aster satellite data on landslide inventory mapping: Yenice-Gökçebey (Western Black Sea Region). MSc thesis, Hacettepe University Graduate School of Science and Engineering, Ankara

ASTM International (2010) ASTM standard D5084. Standard test methods for measurement of hydraulic conductivity of saturated porous materials using a flexible wall permeameter. ASTM International, West Conshohocken, PA. https://doi.org/10.1520/D5084-10

Atalay İ (1997) Türkiye Coğrafyası. Ege Üniversitesi Basımevi, İzmir

Ayalew L (1999) The effect of seasonal rainfall on landslides in the highlands of Ethiopia. Bull Eng Geol Environ 58:9–19

Boll J, Brooks ES, Campbell CR, Stockle CO, Young SK, Hammel JE, McDaniel PA (1998) Progress toward development of a GIS based water quality management tool for small rural watersheds: modification and application of a distributed model. In: Proceedings of the 1998 ASAE Annual International Meeting, Orlando, FL, July 1998. ASAE paper 982230

Bresler E, Russo D, Miller RD (1978) Rapid estimate of unsaturated hydraulic conductivity function. Soil Sci Soc Am J 42:170–177

Calcaterra D, Parise M, Palma B, Pelella L (2000) The influence of meteoric events in triggering shallow landslides in pyroclastic deposits of Campania, Italy. In: Bromhead E, Dixon N, Ibsen ML (eds) Proceedings of the 8th International Symposium on Landslides, Cardiff, Wales, June 2000, Balkema, vol 1, pp 209–214

Canoglu MC (2015) An investigation on the surface water effect in landslide susceptibility mapping: an example from Yenice (Karabük) basin. PhD thesis, Hacettepe University Graduate School of Science and Engineering, Ankara

Canoglu MC (2017) Deterministic landslide susceptibility assessment with the use of a new index (factor of safety index) under dynamic soil saturation: an example from Demirciköy watershed (Sinop/Turkey). Carpathian J Earth Environ Sci 12:423–436

Chung CJF, Fabbri AG (1999) Probabilistic prediction models for landslide hazard mapping. Photogramm Eng Remote Sens 65:1388–1399

Çölkesen İ, Şahin EK, Kavzoglu T (2016) Susceptibility mapping of shallow landslides using kernel-based Gaussian process, support vector machines and logistic regression. J Afr Earth Sci 118:53–64

Demir B, Ercan S (1999) Yenice ilçesindeki heyelanlar üzerine bazı gözlemler. Türkiye 3. Ulusal Heyelan Sempozyumu Özleri Kitabı, Çukurova Üniversitesi, Adana, pp 16–17

Deveciler E (1986) Alaplı-Bartın-Cide (B.Karadeniz) jeoloji raporu, MTA yayınları, Derleme no: 7938, 58 pp

Ercanoglu M (2003) Bulanık mantik ve istatistiksel yontemlerle heyelan duyarlılık haritalarının uretilmesi: Bati Karadeniz Bolgesi (Kumluca Guneyi-Yenice Kuzeyi). PhD thesis, Hacettepe University Graduate School of Science and Engineering, Ankara

Ercanoglu M (2005) Landslide susceptibility assessment of SE Bartın (West Black Sea region, Turkey) by artificial neural networks. Nat Hazards Earth Syst Sci 5:979–992

Ercanoglu M, Gokceoglu C (2002) Assessment of landslide susceptibility for a landslide-prone area (north of Yenice, NW Turkey) by fuzzy approach. Environ Geol 41:720–730

Ercanoglu M, Gokceoglu C (2004) Use of fuzzy relations to produce landslide susceptibility map of a landslide prone area (West Black Sea Region, Turkey). Eng Geol 75:229–250

Ercanoglu M, Gokceoglu C, Van Asch ThWJ (2004) Landslide susceptibility zoning north of Yenice (NW Turkey) by multivariate statistical techniques. Nat Hazards 32:1–23

General Directorate of Natural Disaster (1998) The geological investigation report of Cebeciler landslide. Disaster Investigation and Damage Assessment Agency

General Directorate of Natural Disaster (2000) The geological investigation report of Derebaşı landslide. Disaster Investigation and Damage Assessment Agency

Gérard-Marchant P, Hively WD, Steenhuis TS (2006) Distributed hydrological modelling of total dissolved phosphorus transport in an agricultural landscape, part I: distributed runoff generation. Hydrol Earth Syst Sci 10:245–261

Giannecchini R, Galanti Y, D'Amato Avanzi G (2012) Critical rainfall thresholds for triggering shallow landslides in the Serchio River Valley (Tuscany, Italy). Nat Hazards Earth Syst Sci 12:829–842

Gorsevski PV, Gessler PE, Boll J, Elliot WJ, Foltz RB (2006) Spatially and temporally distributed modeling of landslide susceptibility. Geomorphology 80:178–198

Guzzetti F, Reichenbach P, Cardinali M, Galli M, Ardizzone F (2005) Probabilistic landslide hazard assessment at the basin scale. Geomorphology 72:272–299

Ko FWY, Lo FLC (2016) Rainfall-based landslide susceptibility analysis for natural terrain in Hong Kong—a direct stock-taking approach. Eng Geol 215:95–107

Köppen W (1936) Das geographische System der Klimate, Handbuch der Klimatologie, Bd. 1, Teil C

Kuo WL, Steenhuis TS, McCulloch CE, Mohler CL, Weinstein DA, DeGloria SD, Swaney DP (1999) Effect of grid size on runoff and soil moisture for a variable-source-area hydrology model. Water Resour Res 35:3419–3428

Kuthari S (2007) Establishing precipitation thresholds for landslide initiation along with slope characterisation using GIS-based modelling. MSc thesis, Indian Institute of Remote Sensing (IIRS), Dehradun, India

Lee S, Talib JA (2005) Probabilistic landslide susceptibility and factor effect analysis. Environ Geol 47:982–990

Mead S, Magill C, Hilton J (2016) Rain-triggered lahar susceptibility using a shallow landslide and surface erosion model. Geomorphology 273:168–177

Moore ID, Grayson RB, Ladson AR (1991) Digital terrain modelling: a review of hydrological, geomorphological, and biological applications. Hydrol Process 5:3–30

National Mapping Agency (1999) 1/25000 scaled topographic maps, sheets F28-c1 and F28-b4, Zonguldak, Turkey

Pack RT, Tarboton DG, Goodwin CN (1998) The SINMAP approach to terrain stability mapping. In: Moore D, Hungr O (eds) Proceedings of the 8th International Congress of the International Association for Engineering Geology and the Environment, Vancouver, Canada, September 1998, pp 1157–1165

Pelletier JD, Malamud BD, Blodgett T, Turcotte DL (1997) Scale-invariance of soil moisture variability and its implications for the frequency-size distribution of landslides. Eng Geol 48:255–268

Rawls WJ, Brakensiek DL (1983) A procedure to predict Green and Ampt infiltration parameters. Adv Infilt 12:102–112

Rawls WJ, Brakensiek DL (1985) Prediction of soil water properties for hydrologic modeling. In: Proceedings of a symposium on Watershed Management in the Eighties, Denver, Colorado, April/May 1985, pp 293–299

Ray RL, Jacobs JM, de Alba P (2010a) Impacts of unsaturated zone soil moisture and groundwater table on slope instability. J Geotech Geoenviron Eng 136:1448–1458

Ray RL, Jacobs JM, Cosh MH (2010b) Landslide susceptibility mapping using downscaled AMSR-E soil moisture: a case study from Cleveland Corral, California, US. Remote Sens Environ 114: 2624–2636

Ray RL, Jacobs JM, Ballestero TP (2011) Regional landslide susceptibility: spatiotemporal variations under dynamic soil moisture conditions. Nat Hazards 59:1317–1337

Soil and Water Laboratory (2003) SMDR: the soil moisture distribution and routing model, documentation, version 2.0. Biological and Environmental Engineering Dept., Cornell University, Ithaca, NY

Steenhuis TS, Van Der Molen WH (1986) The Thornthwaite-Mather procedure as a simple engineering method to predict recharge. Journal of Hydrology 84 (3-4):221-229

Süzen ML, Doyuran V (2004) Data driven bivariate landslide susceptibility assessment using geographical information systems: a method and application to Asarsuyu catchment, Turkey. Eng Geol 71:303–321

Süzen ML, Kaya BŞ (2012) Evaluation of environmental parameters in logistic regression models for landslide susceptibility mapping. Int J Digit Earth 5:338–355

Tarboton DG (1997) A new method for the determination of flow directions and upslope areas in grid digital elevation models. Water Resour Res 33:309–319

Temiz N (2000) Batı Karadeniz bölgesi (Bartın, Karabük, Zonguldak yörelerinde) kütle hareketlerinin ve bunları denetleyen jeolojik ve morfolojik özelliklerinin CBS ve Uzaktan Algılama yöntemi ile araştırılması. MSc thesis, Hacettepe University Graduate School of Science and Engineering, Ankara

Thornthwaite CW, Mather JR (1955) The water balance. Technical Report Publication: 8. Drexel Institute of Technology, Laboratory of Climatology, Centerton, New Jersey

Tsangaratos P, Ilia I (2016) Comparison of a logistic regression and Naïve Bayes classifier in landslide susceptibility assessments: the influence of models complexity and training dataset size. CATENA 145:164–179

Van Asch ThWJ, Buma J, Van Beek LPH (1999) A view on some hydrological triggering systems in landslides. Geomorphology 30:25–32

Van Westen CJ, Castellanos E, Kuriakose SL (2008) Spatial data for landslide susceptibility, hazard, and vulnerability assessment: an overview. Eng Geol 102:112–131